Separation Science and Technology
Publication details, including instructions for authors and subscription information:
http://www.informaworld.com/smpp/title~content=t713708471

Adsorption Behavior of Methylene Blue from Aqueous Solution by the Hydrogel Composites Based on Attapulgite

Yi Liu[ab]; Wenbo Wang[a]; Yeling Jin[c]; Aiqin Wang[ac]
[a] Center of Eco-Material and Green Chemistry, Lanzhou Institute of Chemical Physics, Chinese Academy of Sciences, Lanzhou, P. R. China [b] Graduate University of the Chinese Academy of Sciences, Beijing, P. R. China [c] Key Laboratory of Attapulgite Science and Applied Technology of Jiangsu Province, Huaiyin Institute of Technology, Huaian, P. R. China

Online publication date: 26 March 2011

To cite this Article Liu, Yi , Wang, Wenbo , Jin, Yeling and Wang, Aiqin(2011) 'Adsorption Behavior of Methylene Blue from Aqueous Solution by the Hydrogel Composites Based on Attapulgite', Separation Science and Technology, 46: 5, 858 — 868
To link to this Article: DOI: 10.1080/01496395.2010.528502
URL: http://dx.doi.org/10.1080/01496395.2010.528502

Separation Science and Technology, 46: 858–868, 2011

ISSN: 0149-6395 print/1520-5754 online
DOI: 10.1080/01496395.2010.528502

Taylor & Francis
Taylor & Francis Group

Adsorption Behavior of Methylene Blue from Aqueous Solution by the Hydrogel Composites Based on Attapulgite

Yi Liu,[1,3] Wenbo Wang,[1] Yeling Jin,[2] and Aiqin Wang[1,2]

[1]*Center of Eco-Material and Green Chemistry, Lanzhou Institute of Chemical Physics, Chinese Academy of Sciences, Lanzhou, P. R. China*
[2]*Key Laboratory of Attapulgite Science and Applied Technology of Jiangsu Province, Huaiyin Institute of Technology, Huaian, P. R. China*
[3]*Graduate University of the Chinese Academy of Sciences, Beijing, P. R. China*

A series of carboxymethyl cellulose-*g*-poly (acrylic acid)/attapulgite hydrogel composites were synthesized for the removal of cationic dye methylene blue. Various factors affecting the uptake behavior were investigated. Adsorption rate of the hydrogel was quite fast, and adsorption equilibrium could be reached within 30 min. Adsorption kinetics well followed the pseudo-second-order equation for all systems. The Langmuir isotherm was found to best represent the data for the dye uptake. Even when 20 wt% attapulgite was introduced into the hydrogel, the corresponding maximum adsorption capacity reached 1979.48 mg/g at 30°C. The as-prepared adsorbents exhibited excellent affinity for the dye, and can be applied to treat wastewater containing basic dyes.

Keywords adsorption; attapulgite; carboxymethyl cellulose; composite; methylene blue

INTRODUCTION

Some dyes are very toxic pollutants which must be strictly controlled in the water system because of their threat to human physiology and ecological systems even at low concentrations. The presence of even a minute amount of coloring substance in the aquatic system will make it undesirable due to its appearance. Methylene blue (MB) has wider applications due to its good solubility, like coating for paper stock, coloring paper, coloring leather products, dyeing cottons, wools, and temporary hair colorant, etc. Although MB is not strongly hazardous, it can render several harmful effects. Acute exposure to MB will cause increased heart rate, shock, Heinz body formation, vomiting, quadriplegia, cyanosis, jaundice, and tissue necrosis in humans (1,2). It is harmful when it is breathed and in contact with skin and it will be harmful when it is swallowed (3). Accordingly, effluents containing MB and other dyes must be treated before they were discarded. Among existing techniques used for the removal of dyes and other pollutants from wastewater (4), adsorption has been frequently used owing to its facility in design and application (5,6). In addition, the adsorption processes give the best results as they can be used to remove different types and concentrations of dyes, providing an attractive treatment, especially if low-cost adsorbents are used. Many adsorbents have been employed to remove dyes from effluents. Activated carbon is a widely used adsorbent for this purpose as a result of its versatility and porous structure and high adsorption capacity, with the handicaps of being an expensive product and having difficulty in separation from the wastewater after use (7). Consequently, many researchers have diverted to search for more economic and effective adsorbents.

Very recently, the application of hydrogels as adsorbents has been paid special attention. Hydrogels with three-dimensional crosslinked polymeric structures and hydrophilic groups can swell considerably in aqueous solution without dissolution because hydrophilic chains contact one to the other by cross-links (8). Hydrogels have many predominant properties including low interfacial tension and a variety of functional groups which can trap metal ions and ionic dyes like MB from wastewater and endowed hydrogels with high adsorption capacities, which is a favor for the treatment of the environment (9). But pure hydrogels often have some limitations such as low mechanical stability and gel strength and introduction of clays materials into hydrogels can overcome these drawbacks because hydrogels with clays materials combine elasticity and permeability of the gels with high ability of the clays to adsorb different substances (10). As a consequence, much research concerning hydrogels with clays materials adsorbing dyes (11), ammonium nitrogen (12), and metal ions (13) have exponentially increased.

Received 10 May 2010; accepted 28 September 2010.
Address correspondence to Aiqin Wang, Center for Eco-Material and Green Chemistry, Lanzhou Institute of Chemical Physics, Chinese Academy of Sciences, Lanzhou, 730000, China. Tel.: +86 931 4968118; Fax: +86 931 8277088. E-mail: aqwang@licp.cas.cn

Attapulgite (APT), with a fibrous morphology, exchangeable cations, and reactive –OH groups on its surface, is a crystalline hydrated magnesium silicate (14). Carboxymethyl cellulose is an important ether derivative of cellulose and usually used as its sodium salt, which has wide applications (15). Due to its degradation, and being water-soluble, and possessing many functional groups like hydroxyl and carboxymethyl groups, sodium carboxymethyl cellulose (CMC) has attracted great attention. Reactive –OH groups of CMC are used for graft polymerization of hydrophilic vinyl monomers to obtain hydrogels with novel properties.

Based on the background mentioned above, to acquire a novel hydrogel composite with excellent property and low cost, free radical polymerization between CMC, acrylic acid (AA), and APT was carried out and then corresponding hydrogel composites carboxymethyl cellulose-*g*-poly (acrylic acid)/attapulgite (CMC-*g*-PAA/APT) were obtained. The morphology of the composite hydrogel was characterized by Field emission scanning electron microscope (FESEM). To know whether the hydrogel composites have excellent adsorption behavior toward dyes, MB was chosen as representative because of its good affinity for solid surface to investigate the adsorption properties of the as-prepared hydrogel composites toward dyes from aqueous solution. The process parameters affecting the removal amount of MB pertaining to APT content, pH of MB solution, contact time, initial concentration, temperature, and ionic strength were investigated to determine optimum operating conditions. The experimental data were evaluated by applying the pseudo-first-order, pseudo-second-order, and intra-particle diffusion models. The Langmuir, Freundlich, and Tempkin isotherm models were tested for their applicability. The adsorption mechanism was discussed with the assistance of both the adsorbent and the MB loaded adsorbent.

EXPERIMENTAL

Materials

Acrylic acid (AA, chemically pure, monomer, distilled before use), ammonium persulfate (APS, analytical grade, initiator, recrystallized from distilled water before use), and *N*,*N*′-methylenebisacrylamide (MBA, chemical pure, crosslinker, used without further treatment) were purchased from Shanghai Reagent Corp. (Shanghai, China). Sodium carboxymethyl cellulose (CMC, chemical pure, $300 \sim 800\,\text{mPa} \cdot \text{s}$ (25 g/L, 25°C)) was supplied by Sinopharm Chemical Reagent Co., Ltd. (Shanghai, China). Attapulgite (APT) was obtained from Jiangsu Xuyi Junda Aotubang Material Co., Ltd. (Jiangsu, China). Methylene blue (MB) was purchased from Alfa Aesar A Johnson Matthey Company and used as received. The other reagents used were all of analytical reagent grade.

Preparation of CMC-*g*-PAA/APT Hydrogel Composites

CMC-*g*-PAA/APT hydrogel composites were prepared according to our previous report (16). The products were milled and sieved to 80-mesh for further experiment. FTIR spectra indicated that the graft reaction took place among CMC, AA, and APT (16).

MB Uptake Experiments Using Batch Method

Batch sorption experiments were carried out on a thermostatic shaker (THZ-98A) with a constant speed of 120 rpm, 0.025 g adsorbent, and 50 mL tested dye solution.

Effect of APT Content

To optimize the experimental process and decide about the appropriate adsorbent for further experiment, six different APT contents of hydrogel composites were studied. The initial MB concentration was 1000 mg/L, and the pH of the solution was not adjusted. The reaction temperature was 30°C and the reaction duration was 180 min. The suspension was centrifuged at 5000 rpm for 10 min. The initial and final concentrations were analyzed using a Specord 200UV/vis spectrophotometer by monitoring the absorbance changes at a wavelength of maximum absorbance (670 nm). Then the adsorption capacity was calculated according to Eq. (1):

$$q = (C_i - C_f) \times V/W \tag{1}$$

where C_i and C_f represent initial and final concentration of MB solution (mg/L); V is the volume of the MB solution used (L), and W is the mass of adsorbent used in the study (g).

Effect of Initial pH of MB Solution

The chosen adsorbents (APT content of 5 wt% and 20 wt%) with the same amount and the same concentration of MB solution with different pH values ranging from 2 to 9 adjusted by 0.1 M hydrochloric acid or sodium hydroxide dilute solution were put into several conical flasks for 180 min at 30°C. The pH value was measured with a pHS-25 pH-meter.

Adsorption Kinetics

The solution pH was adjusted to 7 and the reaction temperature was maintained at 30°C. The solution was taken at a specified time up to 240 min. To explain the adsorption mechanism and investigate the rate law describing MB adsorbed by the hydrogel composites, the kinetic data were analyzed through three kinetic equations, namely pseudo-first-order, pseudo-second-order, and intra-particle diffusion equations.

The pseudo-first-order model equation is presented as (17):

$$\log(q_{1e} - q_t) = \log q_{1e} - k_1 t/2.303 \tag{2}$$

The pseudo-second-order kinetic equation is given as follows (18):

$$t/q_t = 1/(k_2 q_{2e}^2) + t/q_{2e} \quad (3)$$

The equation for the intra-particle diffusion model is denoted as follows (19):

$$q_t = k_{id} t^{0.5} + C \quad (4)$$

where q_{1e}, q_{2e}, and q_t are the amount of adsorbate removed by the adsorbent at equilibrium and any time, respectively (mg/g); k_1, k_2, and k_{id} represent the pseudo-first-order (min^{-1}), pseudo-second-order (g/(mg min)), and intra-particle diffusion model (mg/(g $min^{0.5}$)) rate constant, respectively.

Adsorption Isotherms at Different Temperatures

Batch tests about the initial concentration and temperature influencing the uptake for MB were conducted at four temperatures (i.e., 30, 40, 50, and 60°C). The initial concentration ranged from 900 to 1200 mg/L for CMC-*g*-PAA and CMC-*g*-PAA/5% APT in which the APT content was 5 wt% and 800 to 1200 mg/L for CMC-*g*-PAA/20% APT and pH value of MB solution was set at 7. All samples were equilibrated for 240 min.

Effect of Ionic Strength

Taking CMC-*g*-PAA/5% APT as representative, six different concentrations of sodium chloride (i.e., 0, 0.01, 0.02, 0.04, 0.08, and 0.16 mol/L) were investigated to determine the effect of ionic strength on adsorption. The initial MB solution concentration was 1000 mg/L and the pH was not adjusted. The temperature was kept at 30°C for 120 min.

Characterization

Infrared spectra of the samples were recorded by a FTIR Spectrophotometer (Thermo Nicolet, NEXUS, USA) in the range of $4000 \sim 400\ cm^{-1}$ using KBr pellet. FESEM micrographs were obtained with a JSM-6701 F field emission scanning electron microscope (JEOL) at 50,000× magnifications after coating the sample with gold film.

RESULTS AND DISCUSSION

FESEM Analysis of the Adsorbents

The morphologies of APT and CMC-*g*-PAA/10% APT were examined and shown in Fig. 1. It is found that APT shows a randomly oriented nano-scale fibril. The diameter of a single fibril is less than 100 nm but its length is about several hundreds of nanometers (Fig. 1(a)). The APT fibril is also observed in the FESEM micrograph of CMC-*g*-PAA/10% APT, suggesting that APT fibril disperses in continuous phase of the hydrogel composite. Meanwhile, the introduction of APT into the hydrogel leads to the coarse surface of the hydrogel, which may benefit from the adsorption.

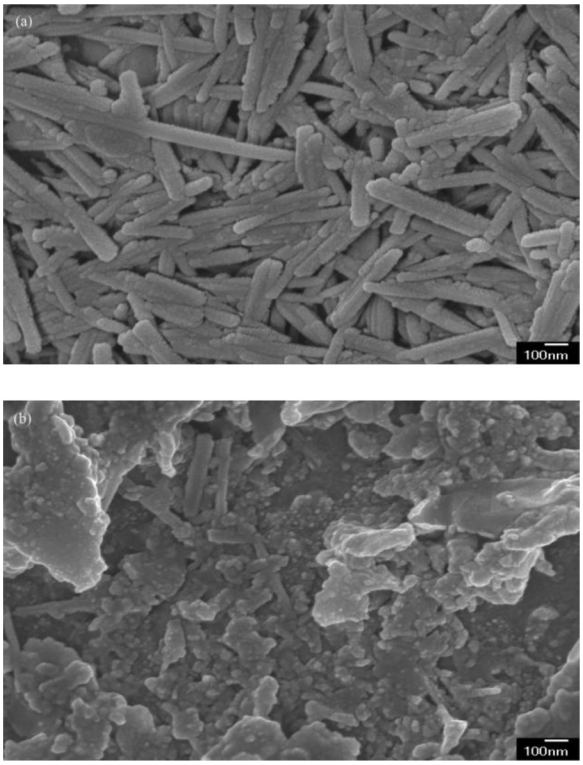

FIG. 1. FESEM micrographs of (a) APT and (b) CMC-*g*-PAA/APT.

Effect of APT Content

The content of clay in the hydrogel was an important parameter which significantly influenced the removal amount of dyes (20). Consequently, the variation of APT content affecting the uptake of MB on the hydrogel composites was investigated, as shown in Fig. 2. As can be seen

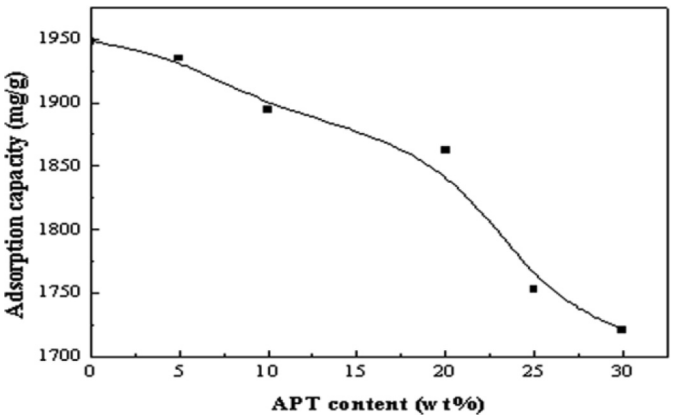

FIG. 2. Variable of APT content on adsorption.

the APT content did influence the adsorption capacities of the adsorbents, and the uptake reduced with increasing APT content. It is known that carboxyl groups on the hydrogel composites dominate the removal of MB from aqueous solution. The introduction of CMC with plenty of groups of $-CH_2COO^-$ into the hydrogel composites, could significantly improve the adsorption properties of the hydrogel composites. Accordingly, even if the hydrogel composite was incorporated into 20 wt% APT, the adsorption capacity of the adsorbent for MB reached 1862.31 mg/g, which distinctly reduced the cost of the adsorbent and enhanced adsorbability for MB and additionally, validated the feasibility of the introduction of CMC into the hydrogel composites.

The change tendency of adsorption capacity along with the APT content resulted from the following reasons. As APT content increased, more APT acted as cross-linking points, and more hydroxyl groups on the APT reacted with carboxyl groups on the CMC or AA, which would consume more carboxyl groups, thus increasing gel intensity (21), correspondingly reducing the uptake of MB. Taking economic cost into account, CMC-*g*-PAA, CMC-*g*-PAA/5% APT, and CMC-*g*-PAA/20% APT were taken as representatives to explore the adsorption properties for MB in detail.

Effect of Initial pH

The initial pH of the solution plays a significant role in the chemistry of the adsorbate and the adsorbent because the change of pH influences the adsorption process through dissociation of functional groups on the active sites of the adsorbent surface and adsorbate (22). It is known that there are lots of –COOH on the backbone of as-prepared hydrogel composites and –OH on the APT, which may be affected by the change of the solution pH. In this case, the effect of pH on the adsorption was performed using various initial solution pH values ($pH = 2 \sim 9$), as shown in Fig. 3. As expected, the uptake of MB increased with the increase of solution pH as the surface became progressively more negatively charged due to deprotonation of the surface, which indicated the pH-dependent adsorption mechanism. However, it seemed that the uptake of MB remained constant in the pH range $4 \sim 9$ for CMC-*g*-PAA and CMC-*g*-PAA/5% APT. When pH was lower than 4, the removal amount of MB showed a significant decrease. But for CMC-*g*-PAA/20% APT, the adsorption capacity appeared to be a constant in the pH range of $7 \sim 9$. When the pH value was lower than 4 the adsorption capacity sharply decreased but when the pH value was within $4 \sim 6$, there was a slight decrease in adsorption capacity. The phenomena possibly attributed to the dissociation constant (pKa) of poly (acrylic acid). The pKa of poly (acrylic acid) is about 4.7 (23), and then the group –COOH can be facilely ionized above the pH value of 4.7,

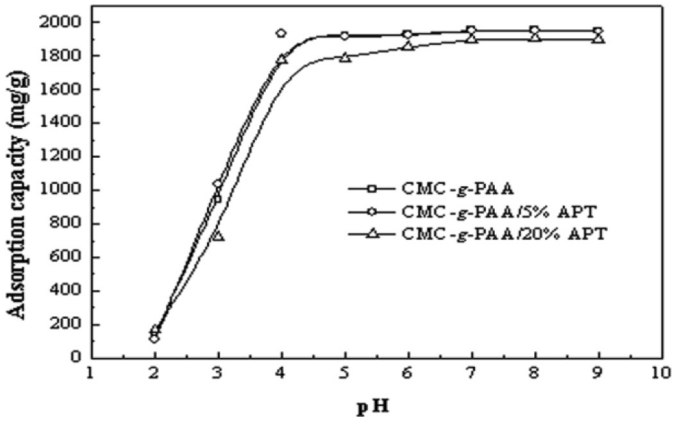

FIG. 3. Effect of initial pH of MB solution on adsorption.

which favors the removal of cationic dye MB. Due to the buffer action of –COOH and $-COO^-$ groups, it may be concluded that the equilibrium adsorption capacity would remain a constant to a certain extent, which was validated in Fig. 3 and mentioned above. At lower pH values, a greater part of the carboxyl groups exists in the form of –COOH, resulting in the decrease of affinity of adsorbent for MB. Accordingly, with the adsorption capacity decreasing, while at high pH, it favors the transformation of –COOH to $-COO^-$, promoting the uptake of MB. However, at lower pH, a part of –COOH is ionized, so a considerable removal amount of MB can be obtained. The optimum pH range for MB removal can be found from Fig. 3, from which it can conclude that the hydrogel composites can be used in a wide pH range.

Effect of Contact Time and Adsorption Kinetics

The adsorption of MB onto the three adsorbents was investigated as a function of contact time to determine the required time for maximum adsorption, and the results were illustrated in Fig. 4. It was clear that the

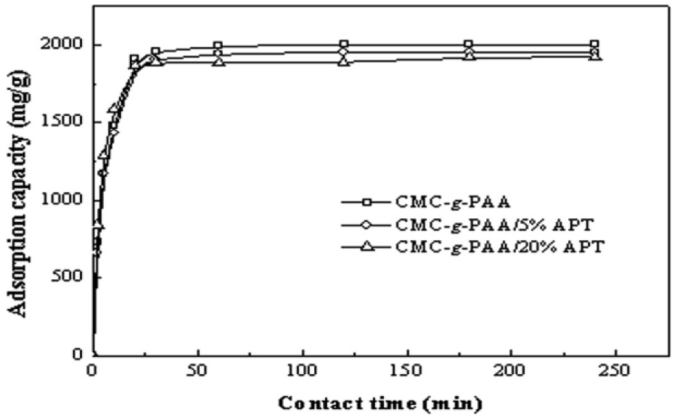

FIG. 4. Effect of contact time on adsorption.

adsorption was quite fast with the increased time from 0 to 20 min, and then progressively slowly increased as time progressed, and reached equilibrium in 30 min. Simultaneously, more than 90% of the equilibrium adsorption capacity occurred within 20 min, which indicated that many vacant activated sites were available for adsorption during the initial stage, thereby making MB prone to contact with the adsorption sites, and thus the removal amount rapidly increasing.

The investigation of adsorption kinetics describes the adsorbate adsorption rate, which dominates the time of adsorbate adsorption at the solid-liquid surface (24). Moreover, adsorption kinetics can provide valuable information on the mechanism of the adsorption process. In this regard, adsorption data were analyzed in terms of pseudo-first-order, pseudo-second-order, and intra-particle diffusion equations, and the related parameters and correlation coefficients obtained from Eqs. (2) and (3) tabulated in Table 1. It can be seen that the relatively higher values of correlation coefficient for pseudo-second-order kinetics than those for pseudo-first-order kinetics indicated that pseudo-second-order expression is the best fit kinetic expression for the entire adsorption process. Though the values of the correlation coefficient in the range of 0.9706 to 0.9864 were acceptable to argue as a best fit, this model fails to explain the sorption saturation (q_{exp}). According to the pseudo-first-order kinetics, the intercept of the plot (q_{1e}) should theoretically represent the sorption saturation for the given condition. In the present study, from Table 1, it can be seen that the values of q_{1e} failed to predicate the values of q_{exp}, while the values of q_{2e} could successfully do so, which indicated the adsorption process of MB onto the adsorbents fitted the pseudo-second-order kinetic model.

For the intra-particle diffusion model Eq. (4) the dependencies of q_t against $t^{0.5}$ were only shown in Fig. 5. It can be seen that the plots consisted of two linear sections with different slopes. The multi-linearity suggested that two or more steps occurred in the sorption process (25). The two linear sections in the root time plots were separately evaluated through Eq. (4), and the corresponding parameters were summarized in Table 2. It was reported that the first straight section was ascribed to macro-pore diffusion and the second linear section was attributed to micro-pore diffusion (26). The value of intercept C reflects thickness of the boundary layer, and the larger the intercept, the greater the thickness of the boundary layer (27). It was clear that the linear line did not pass through the origin, indicating that the intra-particle diffusion was not the only rate-controlling step. The values of the correlation coefficient were lower than those obtained from the pseudo-second-order kinetic model, ascertaining that the pseudo-second-order model reasonably described the dye sorption more accurately.

Effect of Initial Concentration and Adsorption Isotherms

The effect of initial concentration of MB solution on the removal amount of MB by the adsorbents was investigated, as shown in Fig. 6. It was evident that the initial concentration played a significant role in the adsorption process of MB onto the adsorbents. It can be seen that the uptake sharply increased with increasing initial concentration when the concentration was lower than 1050 mg/L, and thereafter gradually increased until it remained unchanged by further increasing the concentration to 1200 mg/L. The results may be ascribed to the following facts. The momentum of the mass transfer would increase with increasing initial concentration, thus bringing on a greater uptake of MB (28). The higher the initial concentration is, the greater the driving force to overcome mass transfer resistance at the solid-liquid surface is. Vacant sites were depleted, which resulted in the adsorption capacity being kept constant when the initial concentration reached a certain limit. Moreover, from Table 3 (1), it was clear that the temperature had a negative effect on the adsorption.

The adsorption isotherms which reflect the interaction between the adsorbate and the adsorbent until a state of equilibrium are important to design and optimize the adsorption system and examine the effectiveness of adsorbent, so it is essential to search for an optimum isotherm model for depicting MB onto applied hydrogel composites. Therefore, the correlation of equilibrium data using either a theoretical or empirical equation is essential for the adsorption interpretation and prediction of the extent of adsorption. In this study, the Langmuir, Freundlich, and Tempkin isotherm models were employed to analyze the adsorption equilibrium data. The Langmuir isotherm model assumes that the adsorption sites on the surface of the adsorbent are identical and the molecules adsorbed do not react with each other. It indicates monolayer coverage of the adsorbate on the adsorbent. The Langmuir equation is given as (29):

$$C_e/q_e = 1/(b \times q_m) + C_e/q_m \quad (5)$$

where C_e is the concentration of adsorbate solution at equilibrium (mg/L); b is the Langmuir constant related to the binding energy of the adsorbent (L/mg); and q_m is the theoretical monolayer saturation adsorption capacity of the adsorbent (mg/g). The values of q_m and b can be determined from the slope and intercept of the plot of C_e/q_e versus C_e.

The essential characteristic of the Langmuir isotherm is expressed in terms of a dimensionless constant called separation factor (R_L), defined by the following equation (30):

$$R_L = 1/(1 + bC_0) \quad (6)$$

TABLE 1
Parameter constants calculated from pseudo-first-order and pseudo-second-order models for MB onto the adsorbents

	Pseudo-first-order model					Pseudo-second-order model			
Samples	Equation	q_{exp} mg/g	q_{1e} mg/g	k_1 min^{-1}	R^2	Equation	q_{2e} mg/g	$k_2 \times 10^{-4}$ g/(mg min)	R^2
CMC-*g*-PAA	$\log (q_{1e} - q_t) = 3.3072–0.0793\ t$	2001.53	2028.76	0.1827	0.9782	$t/q_t = 1.1900 \times 10^{-11} + 4.9305 \times 10^{-4}\ t$	2028.20	2.0428	0.9998
CMC-*g*-PAA/ 5% APT	$\log (q_{1e} - q_t) = 3.3169–0.0849\ t$	1952.46	2074.58	0.1956	0.9706	$t/q_t = 1.2500 \times 10^{-11} + 5.0540 \times 10^{-4}\ t$	1978.62	2.0435	0.9998
CMC-*g*-PAA/ 20% APT	$\log (q_{1e} - q_t) = 3.2763 - 0.0962\ t$	1918.95	1889.25	0.2215	0.9864	$t/q_t = 9.6890 \times 10^{-12} + 5.1723 \times 10^{-4}\ t$	1933.39	2.7611	0.9999

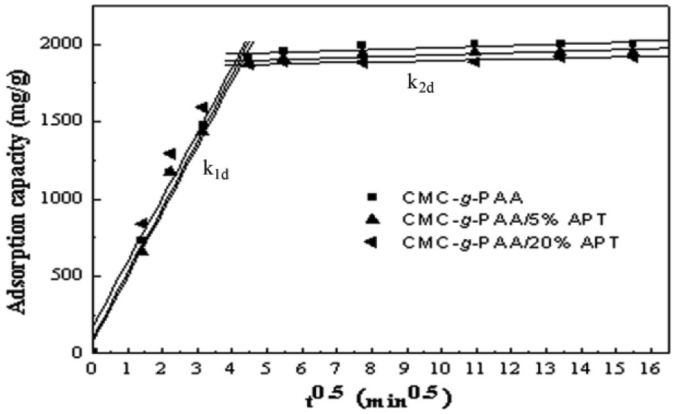

FIG. 5. Intra-particle diffusion plots for MB onto adsorbents. The equations of the first stage are $q_t = 427.74\ t^{0.5} + 92.72$, $q_t = 421.72\ t^{0.5} + 75.00$, $q_t = 419.29\ t^{0.5} + 170.83$, respectively; $q_t = 6.81\ t^{0.5} + 1911.57$, $q_t = 6.35\ t^{0.5} + 1867.52$, $q_t = 4.52\ t^{0.5} + 1848.36$, in the second stage for CMC-*g*-PAA, CMC-*g*-PAA/5% APT, and CMC-*g*-PAA/20% APT, respectively.

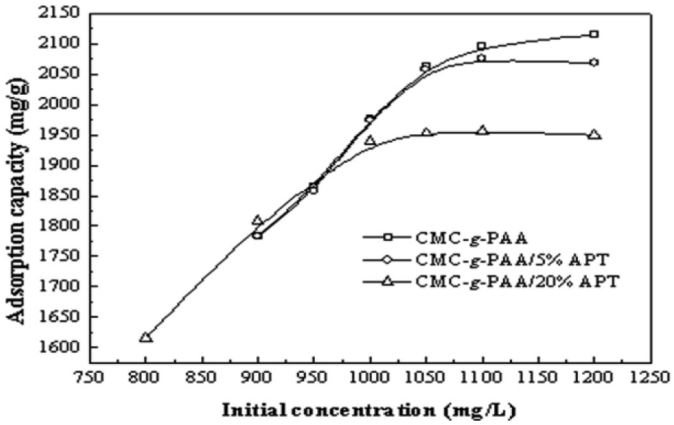

FIG. 6. Effect of initial concentration of MB solution on adsorption.

where C_0 is the initial concentration of the adsorbate solution (mg/L). The value of R_L is an indicator of the type of the isotherm to be either favorable ($0 < R_L < 1$), unfavorable ($R_L > 1$), linear ($R_L = 1$), or irreversible ($R_L = 0$).

In comparison to the Langmuir isotherm, the Freundlich model can be applied to nonideal adsorption on a heterogeneous surface and is generally found to be better suited for the characterization of the multilayer adsorption process indicating that the molecules adsorbed are dependent on each other. The Freundlich equation is empirical. The equation can be written as (31):

$$\ln q_e = \ln K_f + 1/n \ln C_e \tag{7}$$

where K_f represents Freundlich constant ((mg/g)$(L/mg)^{1/n}$), which indicates the adsorption capacity and the strength of the adsorptive bond; $1/n$ is an indicator suggesting the adsorption intensity of adsorbent.

The Tempkin isotherm assumes that the heat of adsorption of all molecules should decrease linearly with the surface coverage due to the existence of the adsorbent-adsorbate interactions. In addition, adsorption is characterized by a uniform distribution of binding energies, up to some maximum binding energy (32). The linear form of the Tempkin isotherm is given as

$$q_e = v \ln(m) + v \ln C_e \tag{8}$$

where v is corresponding to the heat of adsorption (L/g), and m is the dimensionless constant.

By virtue of the Langmuir, Freundlich, and Tempkin isotherm Eqs. (5), (7), and (8) the adsorption equilibrium data were analyzed, and the related parameters were listed in Table 3 (1) and (2), respectively. It can be seen that the values of the correlation coefficient obtained from the Langmuir equation were much higher than those from the Freundlich equation and Tempkin equation at different temperatures. According to the values of the correlation coefficient, the Tempkin isotherm equation represents the poorest fit of experimental data than the other isotherm equations among the analyzed isotherm equations. In addition, it was evident that the calculated q_m values from the Langmuir equation (Eq. (5)) were in accordance with those experimentally determined. Furthermore, constants R_L (Eq. (6)) and $1/n$ lied within the favorable range between 0 and 1. Based on the above analysis, the experimental data were reasonably described by the Langmuir

TABLE 2
Intra-particle diffusion model parameter constants for the adsorption of MB onto the adsorbents

		Intra-particle diffusion model				
Samples	k_{1d} mg/(g $min^{0.5}$)	C mg/g	R^2	k_{2d} mg/(g $min^{0.5}$)	C mg/g	R^2
CMC-*g*-PAA	427.74	92.72	0.9841	6.81	1911.57	0.6649
CMC-*g*-PAA/5% APT	421.72	75.00	0.9818	6.35	1867.52	0.7128
CMC-*g*-PAA/20% APT	419.29	170.83	0.9486	4.52	1848.36	0.8115

TABLE 3
(1) Langmuir and Freundlich models parameters for MB onto the adsorbents

		Langmuir model						Freundlich model			
	t		q_e	q_m	b				K_f		
Samples	°C	Equation	mg/g	mg/g	L/mg	R^2	$R_L \times 10^4$	Equation	(mg/g) $(L/mg)^{1/n}$	1/n	R^2
CMC-*g*-PAA	30	$C_e/q_e = 4.99 \times 10^{-4} + 4.64 \times 10^{-4} C_e$	2116.22	2153.50	0.9306	0.9995	8.9468∼ 11.9255	$\ln q_e = 7.46 + 0.0497 \ln C_e$	1735.59	0.0497	0.2864
	40	$C_e/q_e = 3.94 \times 10^{-4} + 4.72 \times 10^{-4} C_e$	2093.34	2120.32	1.1965	0.9998	6.9599∼ 9.2777	$\ln q_e = 7.44 + 0.0540 \ln C_e$	1706.38	0.0540	0.4834
	50	$C_e/q_e = 4.48 \times 10^{-4} + 4.72 \times 10^{-4} C_e$	2090.09	2119.33	1.0525	0.9999	7.9114∼ 10.5457	$\ln q_e = 7.42 + 0.0571 \ln C_e$	1676.33	0.0571	0.6454
	60	$C_e/q_e = 4.65 \times 10^{-4} + 4.75 \times 10^{-4} C_e$	2074.52	2103.32	1.0232	0.9999	8.1378∼ 10.8474	$\ln q_e = 7.41 + 0.0584 \ln C_e$	1652.23	0.0584	0.6724
CMC-*g*-PAA/ 5% APT	30	$C_e/q_e = 4.98 \times 10^{-4} + 4.77 \times 10^{-4} C_e$	2076.11	2094.80	0.9580	0.9991	8.6911∼ 11.5848	$\ln q_e = 7.48 + 0.0361 \ln C_e$	1768.65	0.0361	0.2072
	40	$C_e/q_e = 4.73 \times 10^{-4} + 4.75 \times 10^{-4} C_e$	2073.62	2103.45	1.0060	0.9994	8.2768∼ 11.0327	$\ln q_e = 7.44 + 0.0486 \ln C_e$	1708.14	0.0486	0.3577
	50	$C_e/q_e = 4.51 \times 10^{-4} + 4.80 \times 10^{-4} C_e$	2063.00	2084.92	1.0633	0.9995	7.8311∼ 10.4387	$\ln q_e = 7.44 + 0.0466 \ln C_e$	1709.46	0.0466	0.3811
	60	$C_e/q_e = 7.32 \times 10^{-4} + 4.76 \times 10^{-4} C_e$	2060.53	2101.21	0.6505	0.9991	12.7943∼ 17.0518	$\ln q_e = 7.37 + 0.0646 \ln C_e$	1587.30	0.0646	0.4603
CMC-*g*-PAA/ 20% APT	30	$C_e/q_e = 1.01 \times 10^{-3} + 5.05 \times 10^{-4} C_e$	1956.50	1979.48	0.5002	0.9994	16.6323∼ 24.9277	$\ln q_e = 7.32 + 0.0551 \ln C_e$	1504.05	0.0551	0.4785
	40	$C_e/q_e = 6.47 \times 10^{-4} + 5.21 \times 10^{-4} C_e$	1932.70	1919.08	0.8057	0.9992	10.3323∼ 15.4904	$\ln q_e = 7.33 + 0.0474 \ln C_e$	1520.43	0.0474	0.3955
	50	$C_e/q_e = 4.88 \times 10^{-4} + 5.30 \times 10^{-4} C_e$	1927.35	1886.52	1.0859	0.9993	7.6682∼ 11.4980	$\ln q_e = 7.32 + 0.0451 \ln C_e$	1515.74	0.0451	0.3824
	60	$C_e/q_e = 9.99 \times 10^{-4} + 5.23 \times 10^{-4} C_e$	1918.24	1912.99	0.5231	0.9997	15.9053∼ 23.8390	$\ln q_e = 7.31 + 0.0480 \ln C_e$	1496.54	0.0480	0.4740

TABLE 3
(2) Tempkin model parameters for MB onto the adsorbents

Samples	t °C	Tempkin model Equation	v L/g	$m \times 10^{-6}$	R^2
CMC-*g*-PAA	30	$q_e = 1722.91 + 98.37 \ln C_e$	98.37	40.44	0.2958
	40	$q_e = 1692.24 + 105.64 \ln C_e$	105.64	9.06	0.4917
	50	$q_e = 1657.19 + 111.81 \ln C_e$	111.81	2.74	0.6579
	60	$q_e = 1631.02 + 113.54 \ln C_e$	113.54	1.73	0.6855
CMC-*g*-PAA/5% APT	30	$q_e = 1762.39 + 70.67 \ln C_e$	70.67	67622	0.2120
	40	$q_e = 1696.59 + 94.45 \ln C_e$	94.45	63.28	0.3629
	50	$q_e = 11697.92 + 90.34 \ln C_e$	90.34	145.23	0.3837
	60	$q_e = 1556.13 + 124.77 \ln C_e$	124.77	0.26	0.4658
CMC-*g*-PAA/20% APT	30	$q_e = 1478.76 + 100.06 \ln C_e$	100.06	2.62	0.4952
	40	$q_e = 1503.97 + 84.55 \ln C_e$	84.55	53.12	0.4044
	50	$q_e = 1502.87 + 79.07 \ln C_e$	79.07	179.79	0.3802
	60	$q_e = 1478.32 + 84.64 \ln C_e$	84.64	38.50	0.4765

model for the entire adsorption process, indicating a monolayer adsorption of MB onto the adsorbents and also the homogeneous distribution of active sites on the adsorbents. Furthermore, the as-prepared adsorbents have higher maximum adsorption capacities q_m than other adsorbents reported (Table 4), which indicated the effectiveness of the adsorbents used in the present work.

Effect of Ionic Strength

Dye adsorption strongly affected by electrostatic parameters such as oxide surface charge, pH, and ionic strength. Consequently, taking CMC-*g*-PAA/5% APT as representative, effect of ionic strength on adsorption of MB onto the adsorbents was investigated, as illustrated in Fig. 7. The uptake of MB decreased as sodium chloride concentration increased. It was largely because of the screening effect that Na^+ partially neutralized the negative surface charge, and then resulted in a compression of the electrical double layer, which led to a reduction in the attractive forces between the surfaces of the adsorbent and the MB cationic species (38).

TABLE 4
Comparison of the maximum adsorption capacity of MB onto different adsorbents

Adsorbents	t (°C)	q_m (mg/g)	References
Raw date pits	20	281	(7)
H-mag	25	173	(33)
Na-mag	25	331	(33)
HA-Am-PAA-B	30	242.4	(34)
CTS-*g*-PAA/10% VMT	30	1682.18	(35)
Polymer modified biomass	25	869.6	(36)
MWS	40	450.0±14.4	(37)
CMC-*g*-PAA	30	2153.50	this work
CMC-*g*-PAA/5% APT	30	2094.80	this work
CMC-*g*-PAA/20% APT	30	1979.48	this work

Adsorption Mechanism

To better understand the adsorption mechanism, FTIR spectra of MB and CMC-*g*-PAA/5% APT before and after adsorption were investigated, as depicted in Fig. 8. The absorption bands at 1609, 1487, and 1453 cm^{-1} (Fig. 8a) were ascribed to the stretching vibration of the C–C bond

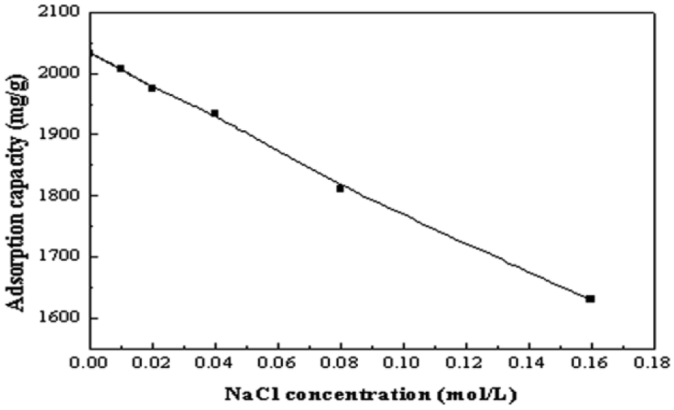

FIG. 7. Effect of ionic strength on adsorption.

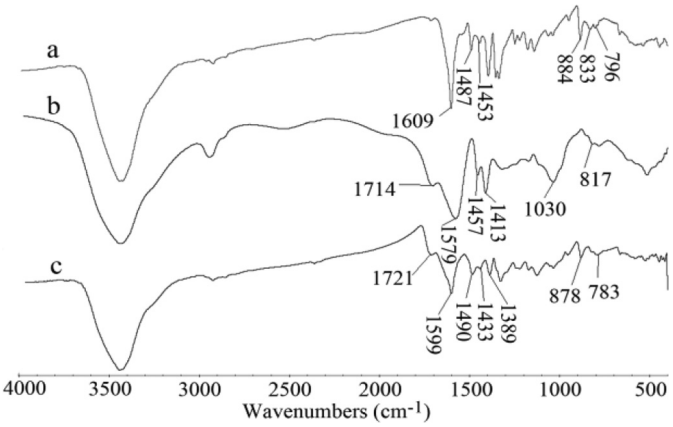

FIG. 8. FTIR spectra of MB (a), CMC-*g*-PAA/5% APT (b), and MB loaded CMC-*g*-PAA/5% APT (c).

in aromatic structure. The bands at 884, 833, and 796 cm^{-1} were corresponding to the characteristic absorption bands of aromatic skeletal groups, which overlapped the absorption band of Si–O bond (817 cm^{-1}) after being adsorbed. All these absorption bands appeared and shifted in the spectra of MB loaded CMC-*g*-PAA/5% APT. The band at 1714 cm^{-1}, related to the stretching vibration of –COOH was shifted to a high wave number after adsorption of MB. The bands at 1457 and 1413 cm^{-1} assigned to $–COO^-$ symmetric stretching and the band at 1579 cm^{-1} ascribed to $–COO^-$ asymmetric stretching were shifted after adsorption (21), which overlapped the absorption bands of the C–C bond in aromatic structure. Based on the above analysis, groups –COOH, $–COO^-$ were involved in the adsorption process of MB onto the adsorbent, which probably indicated that ion exchange and electrostatic attraction were two of the major adsorption mechanisms for binding MB to the hydrogel composite.

CONCLUSIONS

CMC-*g*-PAA/APT hydrogel composites were synthesized and MB was taken as representative to evaluate the adsorption property of the as-prepared adsorbents toward dye. Various factors affecting the uptake behavior were systematically investigated. The adsorption kinetics was in good accordance with the pseudo-second-order equation for all systems studied. The equilibrium data were analyzed by the Langmuir, Freundlich, and Tempkin isotherm equations, and the results showed that the Langmuir isotherm could well describe the adsorption process, and the maximum adsorption capacities calculated from the Langmuir equation showed excellent adsorption properties of the adsorbents. Feasible improvements in the uptake behaviors encourage efforts for the hydrogel composites to be used in wastewater treatment.

ACKNOWLEDGEMENTS

The authors thank the joint support by the National Natural Science Foundation of China (No. 20877077) and Science and the Foundation of Key Laboratory for Attapulgite Science and Applied Technology of Jiangsu Province (No. HPK200901).

REFERENCES

1. Nuhoglu, Y.; Malkoc, E.; Gürses, A.; Canpolat, N. (2002) The removal of Cu(II) from aqueous solutions by *Ulothrix zonata*. *Bioresour. Technol.*, 85 (3): 331.
2. Kumar, K.V.; Ramamurthi, V.; Sivanesan, S. (2005) Modeling the mechanism involved during the sorption of methylene blue onto fly ash. *J. Colloid Interface Sci.*, 284 (1): 14.
3. Inel, O.; Kayikci, N. (1990) Bentonit turu killerde boyar madde adsorpsiyonu. *Doğa-TR. T. Engineering and Environmental Sciences*, 14: 332.
4. Forgacs, E.; Cserháti, T.; Oros, G. (2004) Removal of synthetic dyes from wastewaters: A review. *Environ. Int.*, 30 (7): 953.
5. Wang, X.; Wang, A. (2010) Adsorption characteristics of chitosan-*g*-poly(acrylic acid)/attapulgite hydrogel composite for Hg^{2+} ions from aqueous solution. *Sep. Sci. Technol.*, doi: 10.1080/01496395.2010.504436.
6. Gupta, V.K.; Mohan, D.; Sharma, S.; Sharma, M. (2000) Removal of basic dyes (rhodamine B and methylene blue) from aqueous solutions using bagasse fly ash. *Sep. Sci. Technol.*, 35 (13): 2097.
7. Al-Ghouti, M.A.; Li, J.; Salamh, Y.; Al-Laqtah, N.; Walker, G.; Ahmad, M.N.M. (2010) Adsorption mechanisms of removing heavy metals and dyes from aqueous solution using date pits solid adsorbent. *J. Hazard. Mater.*, 176 (1–3): 510.
8. Sannino, A.; Pappadà, S.; Madaghiele, M.; Maffezzoli, A.; Ambrosio, L.; Nicolais, L. (2005) Crosslinking of cellulose derivatives and hyaluronic acid with water-soluble carbodiimide. *Polymer*, 46 (25): 11206.
9. Yi, J.-Z.; Zhang, L.-M. (2008) Removal of methylene blue dye from aqueous solution by adsorption onto sodium humate/polyacrlamide/clay hybrid hydrogels. *Bioresour. Technol.*, 99 (7): 2182.
10. Öztop, H.N.; Hepokur, C.; Saraydin, D. (2010) Poly(acrylamide/maleic acid)-sepiolite composite hydrogels for immobilization of invertase. *Polym. Bull.*, 64 (1): 27.
11. Kaşgöz, H.; Durmus, A. (2008) Dye removal by a novel hydrogel-clay nanocomposite with enhanced swelling properties. *Polym. Adv. Technol.*, 19 (7): 838.
12. Zheng, Y.; Wang, A. (2009) Evaluation of ammonium removal using a chitosan-*g*-poly (acrylic acid)/rectorite hydrogel composite. *J. Hazard. Mater.*, 171 (1–3): 671.
13. Chen, H.; Wang, A. (2009) Adsorption characteristics of Cu^{2+} from aqueous solution onto poly(acrylamide)/attapulgite composite. *J. Hazard. Mater.*, 165 (1–3): 223.
14. Neaman, A.; Singer, A. (2004) Possible use of the Sacalum (Yucatan) palygorskite as drilling muds. *Appl. Clay Sci.*, 25 (1–2): 121.
15. Li, W.; Sun, B.; Wu, P. (2009) Study on hydrogen bonds of carboxymethyl cellulose sodium film with two-dimensional correlation infrared spectroscopy. *Carbohydr. Polym.*, 78 (3): 454.
16. Wang, W.; Wang, A. (2010) Nanocomposite of carboxymethyl cellulose and attapulgite as a novel pH-sensitive superabsorbent: Synthesis, characterization and properties. *Carbohydr. Polym.*, 82 (1): 83.
17. Lagergren, S.; Svenska, B.K. (1898) Zur theorie der sogenannten adsorption geloester stoffe. *Kungliga Svenska Vetensk. Handl.*, 24 (4): 1.
18. Ho, Y.S.; McKay, G. (1998) Sorption of dye from aqueous solution by peat. *Chem. Eng. J.*, 70 (2): 115.

19. Weber, W.J.; Morris, J.C. (1962) *Proceedings of the International Conference on Water Pollution Symposium*. Pergamon, Oxford. 231.
20. Li, P.; Siddaramaiah, Kim, N.H.; Heo, S.-B.; Lee, J.-H. (2008) Novel PAAm/Laponite clay nanocomposite hydrogels with improved cationic dye adsorption behavior. *Composites Part B*, 39 (5): 756.
21. Zhang, J.; Wang, Q.; Wang, A. (2007) Synthesis and characterization of chitosan-*g*-poly(acrylic acid)/attapulgite superabsorbent composites. *Carbohydr. Polym.*, 68 (2): 367.
22. Zohra, B.; Aicha, K.; Fatima, S.; Nourredine, B.; Zoubir, D. (2008) Adsorption of Direct Red 2 on bentonite modified by cetyltrimethylammonium bromide. *Chem. Eng. J.*, 136 (2–3): 295.
23. Lee, J.W.; Kim, S.Y.; Kim, S.S.; Lee, Y.M.; Lee, K.H.; Kim, S.J. (1999) Synthesis and characteristics of interpenetrating polymer network hydrogel composed of chitosan and poly(acrylic acid). *J. Appl. Polym. Sci.*, 73 (1): 113.
24. Ma, J.; Jia, Y.-Z.; Jing, Y.; Sun, J.-H.; Yao, Y.; Wang, X.-H. (2010) Equilibrium models and kinetic for the adsorption of methylene blue on Co-hectorites. *J. Hazard. Mater.*, 175 (1–3): 965.
25. Wu, F.C.; Tseng, R.L.; Juang, R.S. (2005) Comparisons of porous and adsorption properties of carbons activated by steam and KOH. *J. Colloid Interface Sci.*, 283 (1): 49.
26. Allen, S.J.; McKay, G.; Khader, K.Y.H. (1989) Intraparticle diffusion of a basic dye during adsorption onto sphagnum peat. *Environ. Pollut.*, 56 (1): 39.
27. Sathishkumar, M.; Binupriya, A.R.; Kavitha, D.; Selvakumar, R.; Jayabalan, R.; Choi, J.G.; Yun, S.E. (2009) Adsorption potential of maize cob carbon for 2,4-dichlorophenol removal from aqueous solutions: equilibrium, kinetics and thermodynamics modeling. *Chem. Eng. J.*, 147 (2–3): 265.
28. Hameed, B.H.; Din, A.T.M.; Ahmad, A.L. (2007) Adsorption of methylene blue onto bamboo-based activated carbon: kinetics and equilibrium studies. *J. Hazard. Mater.*, 141 (3): 819.
29. Langmuir, I. (1918) The adsorption of gases on plane surfaces of glass, mica and platinum. *J. Am. Chem. Soc.*, 40 (9): 1361.
30. Hall, K.R.; Eagleton, L.C.; Acrivos, A.; Vermeulen, T. (1966) Pore- and solid-diffusion kinetics in fixed-bed adsorption under constant-pattern conditions. *Ind. Eng. Chem. Fundam.*, 5 (2): 212.
31. Freundlich, H.M.F. (1906) Über die adsorption in lösungen. *Z. Phys. Chem.*, 57A: 385.
32. Tempkin, M.J.; Pyzhev, V. (1940) Recent modification to Langmiur isotherms. *Acta Physiol. Chem.*, 12: 217.
33. Royer, B.; Cardoso, N.F.; Lima, E.C.; Macedo, T.R.; Airoldi, C. (2010) Sodic and acidic crystalline lamellar magadiite adsorbents for the removal of methylene blue from aqueous solutions: kinetics and equilibrium studies. *Sep. Sci. Technol.*, 45 (1): 129.
34. Anirudhan, T.S.; Suchithra, P.S.; Radhakrishnan, P.G. (2009) Synthesis and characterization of humic acid immobilized-polymer/bentonite composites and their ability to adsorb basic dyes from aqueous solutions. *Appl. Clay Sci.*, 43 (3–4): 336.
35. Liu, Y.; Zheng, Y.; Wang, A. (2010) Enhanced adsorption of Methylene Blue from aqueous solution by chitosan-*g*-poly (acrylic acid)/vermiculite hydrogel composites. *Journal of environmental Sciences*, 22 (4): 486.
36. Yu, J.-X.; Li, B.-H.; Sun, X.-M.; Yuan, J.; Chi, R. (2009) Polymer modified biomass of baker's yeast for enhancement adsorption of methylene blue, rhodamine B and basic magenta. *J. Hazard. Mater.*, 168 (2–3): 1147.
37. Han, R.; Zhang, L.; Song, C.; Zhang, M.; Zhu, H.; Zhang, L. (2010) Characterization of modified wheat straw, kinetics and equilibrium study about copper ion and methylene blue adsorption in batch mode. *Carbohydr. Polym.*, 79 (4): 1140.
38. López-Ramón, V.; Moreno-Castilla, C.; Rivera-Utrilla, J.; Radovic, L.R. (2003) Ionic strength effects in aqueous phase adsorption of metal ions on activated carbons. *Carbon*, 41 (10): 2020.